INTERNATIONAL JOURNAL FOR NUMERICAL METHODS IN ENGINEERING, VOL. 40, 3141–3161 (1997)

IMPROVED NUMERICAL METHOD FOR THE TRACTION BOUNDARY INTEGRAL EQUATION BY APPLICATION OF STOKES' THEOREM

A. YOUNG

Structural Materials Centre, Defence Research Agency, Farnborough, Hampshire, GU14 0LX, U.K.

ABSTRACT

This paper concerns the direct numerical evaluation of singular integrals arising in Boundary Integral Equations for displacement (BIE) and displacement gradients (BIDE), and the formulation of a Traction Boundary Integral Equation (TBIE) for solving general elastostatic crack problems. Subject to certain continuity conditions concerning displacements and tractions at the source point, singular integrals in the BIE and the BIDE corresponding to coefficients of displacement and displacement gradients at the source point are shown to be of a form that allows application of Stokes' theorem. All the singular integrals in 3-D BIE and BIDE are reduced to non-singular line integrals, and those in 2-D BIE and BIDE are evaluated in closed form. Remaining terms involve regular integrals, and no references to Cauchy or Hadamard principal values are required. Continuous isoparametric interpolations used on continuous elements local to the source point are modified to include unique displacement gradients at the source point which are compatible with all local tractions. The resulting numerical BIDE is valid for source points located arbitrarily on the boundary, including corners, and a procedure is given for constructing a TBIE from the BIDE. Some example solutions obtained using the present numerical method for the TBIE in 2-D and 3-D are presented.

Int. J. Numer. Meth. Engng., **40**, 3141–3161 (1997)

No. of Figures: 5. No. of Tables: 5. No. of References: 13.

KEY WORDS: traction boundary integral equation; continuous elements; boundary element method; Stokes' theorem; cracks

1. INTRODUCTION

In the Boundary Integral Equations for displacement (BIE) and displacement gradients (the boundary integro-differential equation BIDE), from which the Traction Equation (TBIE) is constructed, there arise apparently singular terms due to the presence of the source point on the boundary surface S. Provided that certain continuity conditions hold for the surface variables (displacement and traction) at the source point, no singularities actually exist and the integral equations are well defined for source points on the boundary. It may be deduced[1] that the general form of these conditions, valid at any boundary point including a corner, requires the assumed forms of the displacement and traction on the boundary to be precisely consistent with unique

Correspondence to: A. Young, Structural Materials Centre, Defence Research Agency, A7 Building, Farnborough, Hampshire, GU14 0LX, U.K.

Received 26 February 1996
Revised 9 August 1996

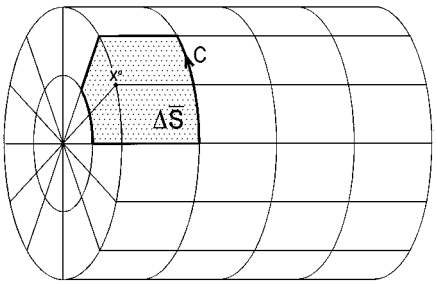

Figure 1. Example of surface $\Delta\bar{S}$ and contour C for a 3-D corner point $\mathbf{x}^0$

(i.e. continuous) displacement gradients at the source point. Conventional isoparametric interpolations between nodal values of displacement and traction do not enforce these conditions at points common to two or more boundary elements, and a special interpolation scheme is required specifically to incorporate the required continuity at the source point. Then, the coefficients of the unique displacements and displacement gradients at the source point may be isolated for special treatment.

The forms of the boundary integral equations may be derived by considering an equivalent surface $S(\varepsilon)$ composed of the open region $\bar{S}$, being the part of S exterior to an infinitesimal sphere of radius ε surrounding the boundary source point, and the infinitesimal region S_ε, being the part of the sphere of radius ε which is interior to S. Then as $\varepsilon \to 0$ and $S(\varepsilon) \to S$, the limiting forms of the BIE and BIDE exist provided that all singular terms, e.g. $O(\log \varepsilon)$ and $O(\varepsilon^{-1})$, cancel out. The contribution from S_ε in the BIDE gives free-terms involving displacement and displacement gradient at the source point, and integrals from $\bar{S}$ are interpreted as Hadamard or Cauchy principal values. All these terms may be computed directly in a boundary element program and used to obtain numerical solutions for crack problems.[1]

A more elegant and computationally more efficient method for dealing with the singular integrals is to apply Stokes' integral theorem over some simply connected part ΔS of the closed boundary $S \equiv \lim_{\varepsilon \to 0} S(\varepsilon)$ surrounding the source point, thereby converting them into non-singular line integrals taken along the remote perimeter C of ΔS for 3-D problems, or non-singular closed-form expressions evaluated at the end points of the arc ΔS for 2-D problems. It is convenient to consider ΔS as consisting of S_ε along with the boundary elements $\Delta\bar{S}$ adjoining the source point (see Figure 1). Stokes' theorem has been used by Cruse *et al.*[2,3] to process certain singular integrals in the BIE and TBIE, and by Mantic[4] on the infinitesimal surface S_ε to derive closed-form expressions for the free term coefficients of displacement in the BIE. However, a more general application of Stokes' theorem is possible for the BIE and the BIDE in elastostatics, analogous to that used by Krishnasamy *et al.*[5] to evaluate source terms in boundary integral equations for potential problems, providing a powerful method for computing the leading source terms directly and accurately. It is shown below that Stokes' theorem may be applied to certain combinations of terms which incorporate all the singular integrals in the BIE and the BIDE (and hence the TBIE). These combinations, expressed as integrals over ΔS, which incorporates the infinitesimal region S_ε, are converted to non-singular expressions and evaluated directly in one simple procedure.

2. BOUNDARY INTEGRAL EQUATIONS

Consider a homogeneous, isotropic, linear elastic solid bounded by the closed surface S, and with shear modulus μ and Poisson's ratio ν. Components of displacement $u_i(\mathbf{x})$, stress $\sigma_{ij}(\mathbf{x})$ and traction $t_i(\mathbf{x}) \equiv \sigma_{ij}(\mathbf{x})n_j(\mathbf{x})$ exist at points $\mathbf{x}$ on the boundary S, where $n_j(\mathbf{x})$ denotes the unit vector in the outward normal direction and the summation convention is assumed for repeated subscripts. Boundary integral equations associated with source (collocation) point $\mathbf{x}^0$ are considered in terms of the relative position vector $\mathbf{r} \equiv \mathbf{x} - \mathbf{x}^0$, and radial distance is given by

$$r = (\mathbf{r}.\mathbf{r})^{1/2} = (r_k r_k)^{1/2} \tag{1}$$

and the derivatives

$$r_{,i} \equiv \frac{\partial r}{\partial x_i} = -\frac{\partial r}{\partial x_i^0} = r_i/r \tag{2}$$

are components of a unit vector. The source point $\mathbf{x}^0$ is taken to be exterior to the equivalent boundary $S(\varepsilon)$, and the main analysis presented below is for the 3-D case, with reference to the 2-D plane strain case where significant differences arise. For simplicity, the forms of the BIE and BIDE are for non-crack problems, and the case of cracks is considered later in Section 5.

The BIE for $\mathbf{x}^0$ exterior to S is

$$I_j(\mathbf{x}^0; S) \equiv \int_S \{T_{ij}(\mathbf{x}, \mathbf{x}^0)u_i(\mathbf{x}) - U_{ij}(\mathbf{x}, \mathbf{x}^0)t_i(\mathbf{x})\}\, \mathrm{d}S(\mathbf{x}) = 0 \tag{3}$$

and its derivative with respect to source position coordinates x_k^0 is the BIDE

$$I_{jk}(\mathbf{x}^0; S) \equiv \frac{\partial}{\partial x_k^0} I_j(\mathbf{x}^0; S) = \int_S \{T_{ijk}(\mathbf{x}, \mathbf{x}^0)u_i(\mathbf{x}) - U_{ijk}(\mathbf{x}, \mathbf{x}^0)t_i(\mathbf{x})\}\, \mathrm{d}S(\mathbf{x}) = 0 \tag{4}$$

The kernel functions for 3-D are given by

$$U_{ij} = \frac{r^{-1}}{16\pi(1-\nu)\mu}\{(3-4\nu)\delta_{ij} + r_{,i}r_{,j}\} \tag{5}$$

$$T_{ij} = \frac{-r^{-2}}{8\pi(1-\nu)}\{r_{,m}n_m[(1-2\nu)\delta_{ij} + 3r_{,i}r_{,j}] + (1-2\nu)[r_{,i}n_j - r_{,j}n_i]\} \tag{6}$$

$$U_{ijk} \equiv \frac{\partial U_{ij}}{\partial x_k^0} = \frac{r^{-2}}{16\pi(1-\nu)\mu}\{(3-4\nu)\delta_{ij}r_{,k} + 3r_{,i}r_{,j}r_{,k} - \delta_{jk}r_{,i} - \delta_{ki}r_{,j}\} \tag{7}$$

$$T_{ijk} \equiv \frac{\partial T_{ij}}{\partial x_k^0} = \frac{r^{-3}}{8\pi(1-\nu)}\{3r_{,m}n_m[\delta_{jk}r_{,i} + \delta_{ki}r_{,j} - (1-2\nu)\delta_{ij}r_{,k} - 5r_{,i}r_{,j}r_{,k}] + 3r_{,i}r_{,j}n_k + (1-2\nu)[\delta_{ij}n_k - (\delta_{jk} - 3r_{,j}r_{,k})n_i + (\delta_{ki} - 3r_{,k}r_{,i})n_j]\} \tag{8}$$

and for 2-D they are

$$U_{ij} = \frac{1}{8\pi(1-\nu)\mu}\{-(3-4\nu)\delta_{ij}\log r + r_{,i}r_{,j}\} \tag{9}$$

$$T_{ij} = \frac{-r^{-1}}{4\pi(1-\nu)}\{r_{,m}n_m((1-2\nu)\delta_{ij} + 2r_{,i}r_{,j}) + (1-2\nu)(r_{,i}n_j - r_{,j}n_i)\} \tag{10}$$

$$U_{ijk} = \frac{r^{-1}}{16\pi(1-\nu)\mu}\{(3-4\nu)\delta_{ij}r_{,k} + 2r_{,i}r_{,j}r_{,k} - \delta_{jk}r_{,i} - \delta_{ki}r_{,j}\} \tag{11}$$

$$T_{ijk} = \frac{r^{-2}}{8\pi(1-\nu)}\{2r_{,m}n_m[\delta_{jk}r_{,i} + \delta_{ki}r_{,j} - (1-2\nu)\delta_{ij}r_{,k} - 4r_{,i}r_{,j}r_{,k}] + 2r_{,i}r_{,j}n_k + (1-2\nu)[\delta_{ij}n_k - (\delta_{jk} - 2r_{,j}r_{,k})n_i + (\delta_{ki} - 2r_{,k}r_{,i})n_j]\} \tag{12}$$

where $n_i \equiv n_i(\mathbf{x})$ and $\delta_{ij} = 1$ if $i = j$ or $= 0$ if $i \neq j$.

In Reference 1, it is deduced that the existence of the BIDE and TBIE for $\mathbf{x}^0$ on S requires the displacement and the displacement gradients to be defined uniquely at the source point, i.e. $u_i(\mathbf{x}^0) = u_i^0$ and $u_{i,j}(\mathbf{x}^0) = u_{i,j}^0$, and the traction $t_i(\mathbf{x}^0)$ on each piecewise smooth part of the surface $\Delta\bar{S}$, having a unique unit outward normal n_i^0 at $\mathbf{x}^0$, to be related to these gradients precisely as

$$t_i(\mathbf{x}^0) = n_j^0 E_{ijkl} u_{k,l}^0 \tag{13}$$

where the elasticity tensor for an isotropic material is of the form

$$E_{ijkl} = \lambda\delta_{ij}\delta_{kl} + \mu(\delta_{ik}\delta_{jl} + \delta_{il}\delta_{jk}) \tag{14}$$

with $\lambda = 2\mu\nu/(1-2\nu)$ for 3-D and 2-D plane strain. Further comments on these continuity requirements are given later in Section 7. Then the two leading terms in series expansions in r about the source point $r = 0$ of the integrands in the BIE and the BIDE may be separated out to give (for 3-D problems)

$$I_j(\mathbf{x}^0; S) = A_{ij}u_i^0 + B_{pqj}u_{p,q}^0 + \int_S O(1)\,\mathrm{d}S \tag{15}$$

$$I_{jk}(\mathbf{x}^0; S) = A_{ijk}u_i^0 + B_{pqjk}u_{p,q}^0 + \int_S O(r^{-1})\,\mathrm{d}S \tag{16}$$

where

$$A_{ij} = \int_{\Delta S} T_{ij}\,\mathrm{d}S \tag{17}$$

$$B_{pqj} = \int_{\Delta S} \{r_q T_{pj} - E_{ispq}n_s U_{ij}\}\,\mathrm{d}S \tag{18}$$

$$A_{ijk} = \int_{\Delta S} T_{ijk}\,\mathrm{d}S = \frac{\partial A_{ij}}{\partial x_k^0} \tag{19}$$

$$B_{pqjk} = \int_{\Delta S} \{r_q T_{pjk} - E_{ispq}n_s U_{ijk}\}\,\mathrm{d}S = \delta_{qk}A_{pj} + \frac{\partial B_{pqj}}{\partial x_k^0} \tag{20}$$

and $\mathrm{d}S \equiv \mathrm{d}S(\mathbf{x})$. For 2-D problems, the residual integrands in (15) and (16) are $O(r)$ and $O(1)$.

In order to enforce uniqueness of displacement gradients at the source point $r = 0$ and satisfaction of the compatibility condition (13), the following special interpolation scheme[1] is used on each piecewise smooth boundary element (having a unique normal n_j^0 at $\mathbf{x}^0$) on $\Delta\bar{S}$

$$u_i(\mathbf{x}) = \bar{u}_i(\xi) + \{u_{i,k}^0 - \bar{u}_{i,k}(\xi^0)\}\rho_k\bar{N}(\mathbf{x}) = u_i^0 + u_{i,k}^0\rho_k + O(r^2) \tag{21}$$

$$t_i(\mathbf{x}) = \bar{t}_i(\xi) + \{n_j^0 E_{ijkl}u_{k,l}^0 - \bar{t}_i(\xi^0)\}\bar{N}(\mathbf{x}) = n_j^0 E_{ijkl}u_{k,l}^0 + O(r) \tag{22}$$

where ξ are intrinsic co-ordinates on the element, with the source point at ξ^0, and $\rho_i \equiv r_i - (r_k n_k^0) n_i^0 = r_i + O(r^2)$ is the projection of r_i onto the tangent plane at $\mathbf{x}^0$. In (21) and (22), the conventional isoparametric interpolations $\bar{u}_i(\xi)$ and $\bar{t}_i(\xi)$, as used on elements exterior to $\Delta\bar{S}$, are modified in the vicinity of the source point using an extra shape function $\bar{N}(\mathbf{x})$ defined on $\Delta\bar{S}$ such that $\bar{N}(\mathbf{x}^0) = 1$. The effects of these modifications are to replace tangential gradients of displacement $\bar{u}_{i,j}(\xi^0)$ at the source point by the parameters $u_{i,j}^0$ and traction $\bar{t}_i(\xi^0)$ at the source point by $n_s^0 E_{ispq} u_{p,q}^0$. Consequently, the proposed interpolation scheme introduces unique values $u_{i,j}^0$ for the displacement gradients at $\mathbf{x}^0$ and allows exact satisfaction of the traction compatibility condition (13) irrespective of which element on $\Delta\bar{S}$ is considered. The extra parameters $u_{i,j}^0$ introduced for this purpose are later to be represented in terms of tractions and displacements on the elements adjoining $\mathbf{x}^0$ when the BIDE is reduced to a TBIE.

When $\Delta\bar{S}$ consists of only one boundary element (i.e. the boundary source point lies inside the perimeter of an element, as for discontinuous elements[6]), the conventional interpolation $\bar{u}_i(\xi)$ already involves unique tangential gradients of displacement at the source point which are independent of the normal gradients implicit in the unique traction $\bar{t}_i(\xi^0)$. Representing the values $u_{i,j}^0$ in terms of displacement and traction on the element ensures that the terms multiplied by $\bar{N}(\mathbf{x})$ in (21) and (22) are identically zero. In this case, using the scheme (21) and (22) merely serves to isolate the coefficients of the gradients $u_{i,j}^0$ for separate treatment, and $\bar{N}(\mathbf{x}) \equiv 1$ may be used.

When $\Delta\bar{S}$ consists of more than one boundary element, the terms multipled by $\bar{N}(\mathbf{x})$ in (21) and (22) are not identically zero, and $\bar{N}(\mathbf{x})$ should be chosen to ensure that the interpolations (21) and (22) match the nodal values of displacement and traction over $\Delta\bar{S}$. The obvious and simplest choice for $\bar{N}(\mathbf{x})$ is the shape function $N^0(\xi)$ associated with the source node on each element, so that $\bar{N}(\mathbf{x}) = 0$ at the non-source node positions and on the remote perimeter C of ΔS. Similar alternative choices for $\bar{N}(\mathbf{x})$ are possible (e.g $N^0(\xi)$ raised to some integer power) and these all produce similar solutions. As more boundary elements are used and the nodal values of displacement and traction converge to the exact elasticity solution, the terms multipled by $\bar{N}(\mathbf{x})$ in (21) and (22), i.e. $\{u_{i,k}^0 - \bar{u}_{i,k}(\xi^0)\}\rho_k$ and $\{n_j^0 E_{ijkl} u_{k,l}^0 - \bar{t}_i(\xi^0)\}$, must tend to zero. Therefore, in principle $\bar{N}(\mathbf{x}) \equiv 1$ could be used for source points common to more than one element, and this is formally equivalent to the equation regularization used by Cruse *et al.*[2] However, in practise this choice produces a less robust numerical method in which convergence of solutions of the TBIE is very erratic, as demonstrated in the numerical results presented later.

Substituting (21) and (22) into (4), the BIDE can be arranged in the form

$$I_{jk}(\mathbf{x}^0; S) = A_{ijk} u_i^0 + C_{pqjk} u_{p,q}^0 + \int_{\Delta S} \{T_{ijk}[\bar{u}_i(\xi) - \bar{u}_i(\xi^0) - \bar{N}(\mathbf{x})\rho_m \bar{u}_{i,m}(\xi^0)] - U_{ijk}[\bar{t}_i(\xi) - \bar{N}(\mathbf{x})\bar{t}_i(\xi^0)]\}\, \mathrm{d}S + \int_{S \setminus \Delta S} \{T_{ijk} u_i(\mathbf{x}) - U_{ijk} t_i(\mathbf{x})\}\, \mathrm{d}S \tag{23}$$

where the coefficients of the displacement gradients are

$$C_{pqjk} = B_{pqjk} + \int_{\Delta S} (\bar{N}(\mathbf{x}) - 1)\{\rho_q T_{pjk} - n_s^0 E_{ispq} U_{ijk}\}\, \mathrm{d}S + \int_{\Delta S} \{(\rho_q - r_q) T_{pjk} - (n_s^0 - n_s) E_{ispq} U_{ijk}\}\, \mathrm{d}S \tag{24}$$

and $n_s E_{ispq} U_{ijk} = \lambda n_m U_{mjk} \delta_{pq} + \mu(n_q U_{pjk} + n_p U_{qjk})$. The integral terms in (23) and (24) other than A_{ijk} and B_{pqjk} are regular, i.e. the integrands are $O(r^{-1})$ in 3-D and $O(1)$ in 2-D, and in these terms the integration range ΔS may be replaced by the boundary elements $\Delta \bar{S}$, since contributions to the regular integrals from the infinitesimal surface S_ε are $O(\varepsilon) \to 0$. The principal computational task involves evaluating the coefficients A_{ijk} and B_{pqjk} of the leading terms, and this is addressed in Sections 3 and 4.

In principle, the BIE could be treated similarly, in which case the surface integrals, other than A_{ij} and B_{pqj}, involve $O(1)$ integrands in 3-D and $O(r)$ integrands in 2-D. However, for the present purposes, the conventional form of the BIE is used

$$I_j(\mathbf{x}^0; S) = A_{ij} u_i^0 + \int_{\Delta S} \{T_{ij}[\bar{u}_i(\xi) - \bar{u}_i(\xi^0)] - U_{ij} \bar{t}_i(\xi)\} \, \mathrm{d}S + \int_{S \setminus \Delta S} \{T_{ij} u_i(\mathbf{x}) - U_{ij} t_i(\mathbf{x})\} \, \mathrm{d}S = 0 \tag{25}$$

with A_{ij} given by (17), and the term B_{pqj} is presented only as a convenient means of deriving B_{pqjk} for the BIDE.

3. STOKES' THEOREM FOR 3-D EQUATIONS

Define the differential operator

$$D_{ij}\{f\} \equiv n_i f_{,j} - n_j f_{,i} \tag{26}$$

where $f(\mathbf{x})$ is any function of position $\mathbf{x}$ on the surface ΔS with unit outward normal $\mathbf{n}$. Then Stokes' theorem states that

$$\int_{\Delta S} D_{ij}\{f\} \, \mathrm{d}S = \varepsilon_{ijk} \oint_C f \, \mathrm{d}x_k \tag{27}$$

where ε_{ijk} is the permutation symbol ($\varepsilon_{ijk} = +1$ if $ijk = 123, 231$ or 312; $\varepsilon_{ijk} = -1$ if $ijk = 321, 213$ or 132; $\varepsilon_{ijk} = 0$ otherwise), and C is the directed line contour describing the perimeter of the surface ΔS such that the vector product $\mathbf{n} \wedge \mathrm{d}\mathbf{x}$ points to the interior of ΔS. In the following analysis, the simply connected open surface ΔS is chosen to be part of the closed surface $S \equiv \lim_{\varepsilon \to 0} S(\varepsilon)$ consisting of the piecewise smooth boundary elements $\Delta \bar{S}$ which adjoin the source point along with the region S_ε on the infinitesimal sphere $r = \varepsilon$.

In the BIE, the kernel (6) may be expressed as follows:

$$T_{ij} = \frac{1}{8\pi(1-\nu)} \left(-(1-2\nu) D_{ij}\{r^{-1}\} + D_{mj}\{r^{-1} r_{,i} r_{,m}\}\right) - \frac{\delta_{ij}}{4\pi} r_{,m} n_m / r^2 \tag{28}$$

so that by applying Stokes' theorem (27),

$$A_{ij} = \int_{\Delta S} T_{ij} \, \mathrm{d}S = \frac{1}{8\pi(1-\nu)} \oint_C r^{-1} \{-(1-2\nu)\varepsilon_{qij} + \varepsilon_{qmj} r_{,i} r_{,m}\} \, \mathrm{d}r_q + \frac{1}{4\pi} \Theta(\mathbf{x}^0) \delta_{ij} \tag{29}$$

where

$$\Theta(\mathbf{x}^0) = -\int_{\Delta S} \frac{r_{,m} n_m}{r^2} \, \mathrm{d}S = \theta - \int_{\Delta \bar{S}} \frac{r_{,m} n_m}{r^2} \, \mathrm{d}S \tag{30}$$

is the solid angle subtended at $\mathbf{x}^0$ by the surface ΔS. The integrand in (29) is non-singular since $r > 0$ on C, and the remaining surface integral $\Theta(\mathbf{x}^0)$ defined in (30) may be evaluated by subdividing ΔS into $\Delta\bar{S}$ and S_ε. On $\Delta\bar{S}$, the integrand in (30) is $O(r^{-1})$ and its contribution is evaluated using standard numerical techniques.[7] On S_ε, $r_{,m} = -n_m$ and its contribution to (30) is the solid angle θ occupied by the volume interior to S at the source point, and this may be calculated from the known tangent vectors to edges of the adjoining boundary elements.[4]

The coefficients (18) of $u^0_{p,q}$ are given by

$$B_{pqj} = \int_{\Delta S} \{r_q T_{pj} - \lambda\delta_{pq} n_m U_{mj} - \mu(n_q U_{pj} + n_p U_{qj})\}\, \mathrm{d}S \tag{31}$$

Substituting the kernels (5) and (6) into (31) and applying Stokes' theorem (27) gives (after some rearrangement of terms)

$$\begin{aligned} B_{pqj} &= \frac{1}{16\pi(1-\nu)} \int_{\Delta S} \Big\{ D_{mp}\{r_{,q} r_{,j} r_{,m}\} + D_{mq}\{r_{,p} r_{,j} r_{,m}\} + 2(1-2\nu) D_{jp}\{r_{,q}\} \\ &\quad + (3-4\nu)\,\delta_{pj} D_{mq}\{r_{,m}\} + \delta_{qj} D_{mp}\{r_{,m}\} + \frac{2(1-\nu)}{1-2\nu}\,\delta_{pq} D_{mj}\{r_{,m}\} \Big\}\, \mathrm{d}S \\ &= \frac{1}{16\pi(1-\nu)} \oint_C \Big\{ \varepsilon_{imp} r_{,q} r_{,j} r_{,m} + \varepsilon_{imq} r_{,p} r_{,j} r_{,m} + 2(1-2\nu)\varepsilon_{ijp} r_{,q} \\ &\quad + (3-4\nu)\delta_{pj}\varepsilon_{imq} r_{,m} + \delta_{qj}\varepsilon_{imp} r_{,m} + \frac{2(1-\nu)}{(1-2\nu)}\,\delta_{pq}\varepsilon_{imj} r_{,m} \Big\}\, \mathrm{d}r_i \end{aligned} \tag{32}$$

On account of the following two identities:

$$\frac{\partial}{\partial x^0_k}(n_m r_{,m}/r^2) = -D_{mk}\{r_{,m}/r^2\} \tag{33}$$

$$\begin{aligned} \frac{\partial}{\partial x^0_k} \int_{\Delta S} D_{pq}\{f(\mathbf{r})\}\, \mathrm{d}S &= \varepsilon_{ipq} \frac{\partial}{\partial x^0_k} \oint_C f(\mathbf{r})\, \mathrm{d}x_i \\ &= \varepsilon_{ipq} \oint_C \frac{\partial f}{\partial x^0_k}\, \mathrm{d}x_i = -\varepsilon_{ipq} \oint_C \frac{\partial f}{\partial r_k}\, \mathrm{d}r_i \end{aligned} \tag{34}$$

the coefficients (19) and (20) in the BIDE may be derived directly from the non-singular expressions (29) and (32)

$$\begin{aligned} A_{ijk} = \frac{\partial A_{ij}}{\partial x^0_k} &= \frac{1}{8\pi(1-\nu)} \oint_C r^{-2} \{3\varepsilon_{qmj} r_{,m} r_{,i} r_{,k} - (1-2\nu)\varepsilon_{qij} r_{,k} + \varepsilon_{qjk} r_{,i} \\ &\quad + 2(1-\nu)\,\delta_{ij}\varepsilon_{qmk} r_{,m} - \delta_{ik}\varepsilon_{qmj} r_{,m}\}\, \mathrm{d}r_q \end{aligned} \tag{35}$$

$$B_{pqjk} = \delta_{qk} A_{pj} + \frac{\partial B_{pqj}}{\partial x_k^0}$$

$$= \frac{1}{16\pi(1-\nu)} \oint_C r^{-1} \Big\{ 3\varepsilon_{imp} r_{,q} r_{,j} r_{,k} r_{,m} + 3\varepsilon_{imq} r_{,p} r_{,j} r_{,k} r_{,m} + 2(1-2\nu)\varepsilon_{ijp} r_{,q} r_{,k}$$
$$- \varepsilon_{ikp} r_{,q} r_{,j} - \varepsilon_{ikq} r_{,p} r_{,j} - \delta_{qk}(\varepsilon_{imp} r_{,j} r_{,m} - 2\varepsilon_{imj} r_{,p} r_{,m})$$
$$- \delta_{jk}(\varepsilon_{imp} r_{,q} r_{,m} + \varepsilon_{imq} r_{,p} r_{,m}) - \delta_{pk} \varepsilon_{imq} r_{,j} r_{,m}$$
$$- (3-4\nu)\delta_{pj}(\varepsilon_{ikq} - \varepsilon_{imq} r_{,m} r_{,k}) - \delta_{qj}(\varepsilon_{ikp} - \varepsilon_{imp} r_{,m} r_{,k})$$
$$- \frac{2(1-\nu)}{1-2\nu} \delta_{pq}(\varepsilon_{ikj} - \varepsilon_{imj} r_{,m} r_{,k}) \Big\} \mathrm{d}r_i + \frac{1}{4\pi} \Theta(\mathbf{x}^0) \delta_{pj} \delta_{qk} \tag{36}$$

4. STOKES' THEOREM FOR 2-D EQUATIONS (PLANE STRAIN)

A 2-D version of Stokes' theorem with coordinates (x_1, x_2) may be derived as a special case of the 3-D equation (27) where $f(\mathbf{x})$ does not vary with x_3 and ΔS is a projection of the 2-D (x_1, x_2) boundary are PQ through x_3

$$\int_P^Q D_{ij}\{f\} \, \mathrm{d}S = \varepsilon_{ij3} [f]_P^Q \equiv \varepsilon_{ij3}(f(Q) - f(P)) \tag{37}$$

Then, for the 2-D kernel (10),

$$T_{ij} = \frac{1}{4\pi(1-\nu)} ((1-2\nu) D_{ij}\{\log r\} + D_{mj}\{r_{,i} r_{,m}\}) - \frac{\delta_{ij}}{2\pi} r_{,m} n_m / r \tag{38}$$

so that the integral (17) may be reduced to the non-singular expression

$$A_{ij} = \frac{1}{4\pi(1-\nu)} [(1-2\nu)\varepsilon_{ij3} \log r + \varepsilon_{mj3} r_{,i} r_{,m}]_P^Q + \frac{1}{2\pi} \delta_{ij} \Theta(\mathbf{x}^0) \tag{39}$$

Owing to the identity $n_m \, \mathrm{d}S = \varepsilon_{mk3} \, \mathrm{d}r_k$, the solid angle term reduces to

$$\Theta(\mathbf{x}^0) = -\int_{\Delta S} \frac{r_{,m} n_m}{r} \mathrm{d}S = \int_{\Delta S} \frac{r_2 \, \mathrm{d}r_1 - r_1 \, \mathrm{d}r_2}{r^2} = [\tan^{-1}(r_1/r_2)]_P^Q \tag{40}$$

and may be evaluated directly in terms of radial vectors directed at the ends P and Q of the arc ΔS, e.g. using $r^P r^Q \cos\Theta = r_1^P r_1^Q + r_2^P r_2^Q$ and $r^P r^Q \sin\Theta = r_1^Q r_2^P - r_2^Q r_1^P$.
The second term (18) reduces to

$$B_{pqj} = \frac{1}{8\pi(1-\nu)} \int_P^Q \Big\{ D_{mp}\{r_{,q} r_{,j} r_m\} + D_{mq}\{r_{,p} r_{,j} r_m\} - 2(1-2\nu) D_{jp}\{r_q \log r\}$$
$$+ (3-4\nu)\delta_{pj} D_{mq}\{r_m(1 - \log r)\} + \delta_{qj} D_{mp}\{r_m(1 - \log r)\}$$
$$+ \frac{2(1-\nu)}{1-2\nu} \delta_{pq} D_{mj}\{r_m(1 - \log r)\} \Big\} \mathrm{d}S$$

$$= \frac{1}{8\pi(1-\nu)} \left[\varepsilon_{mp3} r_{,q} r_{,j} r_m + \varepsilon_{mq3} r_{,p} r_{,j} r_m - 2(1-2\nu)\varepsilon_{jp3} r_q \log r \right.$$
$$\left. + \left\{ (3-4\nu)\delta_{pj}\varepsilon_{mq3} + \delta_{qj}\varepsilon_{mp3} + \frac{2(1-\nu)}{1-2\nu}\,\delta_{pq}\varepsilon_{mj3} \right\} r_m (1 - \log r) \right]_P^Q \tag{41}$$

Then, using the 2-D identities analogous to (33) and (34)

$$\frac{\partial}{\partial x_k^0}\,(n_m r_{,m}/r) = -\,D_{mk}\,\{r_{,m/r}\} \tag{42}$$

$$\frac{\partial}{\partial x_k^0} \int_{\Delta S} D_{pq}\,\{f(\mathbf{r})\}\,\mathrm{d}S = -\,\varepsilon_{pq3} \left[\frac{\partial f}{\partial r_k} \right]_P^Q \tag{43}$$

the following closed-form expressions are obtained

$$A_{ijk} = \frac{\partial A_{ij}}{\partial x_k^0} = \frac{1}{4\pi(1-\nu)} \left[2\varepsilon_{mj3} r_{,m} r_{,i} r_{,k}/r - (1-2\nu)\varepsilon_{ij3} r_{,k}/r + \varepsilon_{jk3} r_{,i}/r \right.$$
$$\left. + 2(1-\nu)\delta_{ij}\varepsilon_{mk3} r_{,m}/r - \delta_{ik}\varepsilon_{mj3} r_{,m}/r \right]_P^Q \tag{44}$$

$$B_{pqjk} = \delta_{qk} A_{pj} + \frac{\partial B_{pqj}}{\partial x_k^0}$$
$$= \frac{1}{8\pi(1-\nu)} \left[2\varepsilon_{mp3} r_{,q} r_{,j} r_{,k} r_{,m} + 2\varepsilon_{mq3} r_{,p} r_{,j} r_{,k} r_{,m} + 2(1-2\nu)\varepsilon_{jp3} r_{,q} r_{,k} \right.$$
$$- \varepsilon_{kq3} r_{,p} r_{,j} - \varepsilon_{kp3} r_{,q} r_{,j} - \delta_{qk}(\varepsilon_{mp3} r_{,j} r_{,m} - 2\varepsilon_{mj3} r_{,p} r_{,m})$$
$$- \delta_{jk}(\varepsilon_{mp3} r_{,q} r_{,m} + \varepsilon_{mq3} r_{,p} r_{,m}) - \delta_{pk}\varepsilon_{mq3} r_{,j} r_{,m}$$
$$- (3-4\nu)\delta_{pj}(\varepsilon_{qk3} \log r - \varepsilon_{mq3} r_{,k} r_{,m}) - \delta_{qj}(\varepsilon_{pk3} \log r - \varepsilon_{mp3} r_{,k} r_{,m})$$
$$\left. - \frac{2(1-\nu)}{1-2\nu}\,\delta_{pq}(\varepsilon_{jk3} \log r - \varepsilon_{mj3} r_{,k} r_{,m}) \right]_P^Q + \frac{1}{2\pi}\,\Theta(\mathbf{x}^0)\delta_{pj}\delta_{qk} \tag{45}$$

5. THE TRACTION BOUNDARY INTEGRAL EQUATION

A formula for defining a generally applicable TBIE from the BIDE (23) has been presented for 3-D problems in Reference 1. A corresponding account of the formulation of a TBIE for 2-D problems is described below. The aim is to reduce the BIDE (four components) to a TBIE (two components) which contain strong free terms involving all traction values at the source (collocation) point $\mathbf{x}^0$. In this reduction, the unique gradient parameters $u_{p,q}^0$ are combined into tractions $n_j^0 E_{ijkl} u_{k,l}^0$, as in (13), and the values $t_i(\mathbf{x}^0)$ previously removed by the special interpolation scheme (22) are restored.

When $\mathbf{x}^0$ is not on the locus of a crack, the four BIDE are of the form

$$I_{kl}(\mathbf{x}^0; S) = C_{pqkl} u_{p,q}^0 + \{\text{terms involving } \mathbf{u} \text{ and } \mathbf{t} \text{ on } S\} = 0 \tag{46}$$

Multiplying (46) by $E_{ijrs} Q_{klrs}$, where E_{ijrs} is defined in (14) and Q_{klrs} are inverse coefficients of C_{pqkl} such that $C_{pqkl} Q_{klrs} = \delta_{pr}\delta_{qs}$, the leading terms $C_{pqkl} u_{p,q}^0$ are combined into stress

components at the boundary source point

$$E_{ijrs}Q_{klrs}C_{pqkl}u^0_{p,q} = E_{ijpq}u^0_{p,q} = \sigma^0_{ij} \tag{47}$$

Then, contracting (47) with a unit vector n^0_j gives the traction t^0_i acting on an element with outward normal n^0_j. However at a 2-D corner, two such elements and normals exist and two corresponding TBIEs may be constructed, each biased towards information concerning its own traction at the expense of the other. The general algebraic form of a TBIE which is capable of considering any loading state should incorporate equally information about all tractions acting on elements adjoining the source point. This inevitably leads to a definition of the TBIE which involves an average of all such traction values

$$\hat{n}_m E_{jmrs}Q_{klrs}I_{kl}(\mathbf{x}^0; S) = \sum_e t^{(e)}_j(\mathbf{x}^0) + \{\text{terms involving } \mathbf{u} \text{ and } \mathbf{t} \text{ on } S\} = 0 \tag{48}$$

where the summation over e refers to the boundary elements $\Delta\bar{S}$ adjoining $\mathbf{x}^0$, and $\hat{n}_m = \sum_e n^{(e)}_m(\mathbf{x}^0)$ is the sum of all unit outward normal vectors at $\mathbf{x}^0$.

The case where $\mathbf{x}^0$ is on the locus of a crack is somewhat more complicated due to the presence of two sets of free terms (one set from each crack face), and the BIDE is of the form

$$\begin{aligned} I_{kl}(\mathbf{x}^0; S) = {} & (C^+_{pqkl}u^{0+}_{p,q} + C^-_{pqkl}u^{0-}_{p,q}) \\ & + \{\text{terms involving only } \mathbf{u}^+ - \mathbf{u}^- \text{ and } \mathbf{t}^+ + \mathbf{t}^- \text{ on cracks}\} \\ & + \{\text{terms involving } \mathbf{u} \text{ and } \mathbf{t} \text{ on non-crack parts of } S\} = 0 \end{aligned} \tag{49}$$

where superscripts $\pm$ refer to quantities associated with opposite crack faces. A TBIE may be used to obtain numerical solutions for the opening displacement $\mathbf{u}^+ - \mathbf{u}^-$ along the crack provided that its free term contains strong information about the traction difference (or crack pressure) $\mathbf{t}^+ - \mathbf{t}^-$, which is otherwise absent (crack pressure terms are entirely absent in the BIE). Such a TBIE may be constructed analogously to (48) by defining the quantities Q_{klrs} such that $\frac{1}{2}(C^+_{pqkl} + C^-_{pqkl})Q_{klrs} = \delta_{pr}\delta_{qs}$, and by taking $\hat{n}_m$ as the sum of normal vectors on either one of the (oppositely orientated) crack faces. However, it is not generally possible to combine all eight displacement gradient free terms in the four BIDE (49) into only crack pressure values, and residual free terms involving $u^+_{p,q} - u^-_{p,q}$ persist in the TBIE, which is of the form

$$\begin{aligned} \hat{n}_m E_{jmrs}Q_{klrs}I_{kl}(\mathbf{x}^0; S) = {} & \sum_e (t^{0+}_j - t^{0-}_j) \\ & + \tfrac{1}{2}\hat{n}_m E_{jmrs}Q_{klrs}(C^+_{pqkl} - C^-_{pqkl})(u^{0+}_{p,q} - u^{0-}_{p,q}) \\ & + \{\text{terms involving } \mathbf{u}^+ - \mathbf{u}^- \text{ and } \mathbf{t}^+ + \mathbf{t}^- \text{ only on cracks}\} \\ & + \{\text{terms involving } \mathbf{u} \text{ and } \mathbf{t} \text{ on non-crack parts of } S\} = 0 \end{aligned} \tag{50}$$

In a boundary element formulation, the residual displacement gradients in the TBIE (50) must be represented in terms of nodal values of displacement and traction on the elements adjoining $\mathbf{x}^0$. Displacement gradients $u^0_{p,q}$ on a smooth section of the boundary may be determined from the traction and the tangential gradient of $\bar{u}_i(\xi)$; at the junction of two elements, the tangential gradients may not match and an average is taken. When required at a corner point, full use is made of all traction values, since these convey direct information about the stress boundary

conditions imposed on the displacement gradients. Values of the displacement gradients $u^0_{p,q}$ at a corner point may be expressed in terms of nodal displacements and tractions as follows. Unique stress components are determined directly from the two traction vectors acting at the corner point, and a unique rotation $u^0_{1,2} - u^0_{2,1}$ is defined from tangential gradients calculated using the conventional interpolation $\bar{u}_i(\xi)$. In terms of normal $\mathbf{n}^e$ and tangential $\hat{\rho}^e$ unit base vectors on each element ($e = 1, 2$) at a corner, the values of the gradients at $\mathbf{x}^0 = \mathbf{x}(\xi^e)$ are determined from the following four conditions (51) to (53). The normal tractions on each element define two tensile stress components ($e = 1, 2$)

$$n^e_i n^e_j E_{ijkl} u^0_{k,l} = n^e_i \bar{t}^e_i(\xi^e) \tag{51}$$

and the corresponding shear stress component is incorporated in

$$n^1_i n^2_j E_{ijkl} u^0_{k,l} = \tfrac{1}{2}(n^1_i \bar{t}^2_i(\xi^2) + n^2_i \bar{t}^1_i(\xi^1)) \tag{52}$$

Ideally, the two terms $n^1_i \bar{t}^2_i(\xi^2)$ and $n^2_i \bar{t}^1_i(\xi^1)$ occurring on the right-hand side of (52) should represent the same stress component, and this is usually the case if tractions are specified as boundary conditions (e.g. on the surfaces of a crack); however, tractions from a numerical solution may not satisfy this condition and so the two values are averaged to give a symmetric formula. Rotation about the corner point is given by

$$(\hat{\rho}^1_1 \hat{\rho}^2_2 - \hat{\rho}^1_2 \hat{\rho}^2_1)\,(u^0_{1,2} - u^0_{2,1}) = \hat{\rho}^1_i D^2_i - \hat{\rho}^2_i D^1_i \tag{53}$$

where $D^e_i \equiv \mathrm{d}\bar{u}^e_i/\mathrm{d}s$ is evaluated at $\mathbf{x}^0 = \mathbf{x}(\xi^e)$ on element e. Using values of $u^0_{i,j}$ determined as above (e.g. using (51) to (53) for corner points), the TBIE may be defined from the BIDE as $\hat{n}_m E_{jmrs} Q_{klrs} I_{kl}(\mathbf{x}^0; S)$ for both the non-crack case (46) and the crack case (49).

Solutions for the opening displacement $\mathbf{u}^+ - \mathbf{u}^-$ over the interior of a crack may be obtained using only the TBIE for source points collocated on the crack locus.[2] However, source points located where a crack intersects with a non-crack boundary require two equations, since separate $\mathbf{u}^+$ and $\mathbf{u}^-$ contributions arise from the non-crack parts of S. For simplicity, the present method determines a complete solution for displacement on both crack surfaces by applying the BIE and TBIE at collocation points on the crack locus, as in the dual boundary element method.[6]

6. NUMERICAL RESULTS

Below is presented a set of examples for which solutions have been obtained using the present boundary element method for the TBIE in 2-D and in 3-D. In all cases, continuous quadratic boundary elements are used. For crack problems, both the BIE and the TBIE are used on the crack locus, and the BIE is used at crack tips and on non-crack surfaces. Quarter point elements are used at crack tips, and values of stress intensity factor are calculated from the crack opening displacement using the formula given in Reference 1 (applicable to 3-D and 2-D plane strain). In the numerical examples, values of shear modulus $\mu = 1{\cdot}0$ and Poisson's ratio $\nu = 0{\cdot}3$ are taken, and for the 2-D examples a state of plane strain is assumed. For the main set of results below, the extra shape function $\bar{N}(\mathbf{x})$ used in the TBIE is chosen to be the shape function $N^0(\xi)$ associated with the source node on each element of $\Delta\bar{S}$. Comments are also given on numerical solutions obtained using $\bar{N}(\mathbf{x}) \equiv 1$ and $\bar{N}(\mathbf{x}) \equiv (N^0(\xi))^2$.

6.1. Circular hole in a rectangular solid under tension (2-*D*)

A rectangular solid $-W \leqslant x_1 \leqslant +W$, $-L \leqslant x_2 \leqslant +L$ containing a central circular hole of radius R is loaded in tension $\mathbf{t} = (0, \pm\sigma)$ on $x_2 = \pm L$. Dimensions chosen are $W = 2{\cdot}0$, $L = 4{\cdot}0$, $R = 0{\cdot}5$, and loading is $\sigma = 1{\cdot}0$. One-quarter of the structure (see Figure 2) is analysed, with symmetry boundary conditions applied on the co-ordinate axes, and solutions from the BIE and the TBIE are compared using values of displacement u_1 at (0·5, 0·0) and u_2 at (0·0, 0·5), and traction t_2 (stress concentration) at (0·5, 0·0). Five meshes are considered, comprising uniform elements of length ℓ on all the straight boundary sections and N elements, each of length $\pi/(4N)$, on the hole quadrant, giving a total of $22{\cdot}0/\ell + N$ elements. The values of ℓ and N chosen are: 0·5 and 2 (24 elements), 0·25 and 3 (47 elements), 0·1667 and 6 (94 elements), 0·125 and 12 (188 elements), 0·0625 and 24 (376 elements). Numerical results are given in Table I, along with the percentage difference between BIE and TBIE solution values, and it may be seen that solutions to both equations converge steadily to the same result, e.g. the stress concentration is about 3·25; the reference value[8] for $R/W = 0{\cdot}25$, $L \gg W$ is 3·24 (accuracy unknown).

In this and similar studies, it is found that displacement values from BIE solutions are typically more accurate than those from TBIE solutions, while traction values from the TBIE solutions are more accurate than those from BIE solutions. This is perhaps not surprising considering the nature of the source terms in the BIE and the TBIE. Using $\bar{N}(\mathbf{x}) \equiv (N^0(\xi))^2$, the solution to the TBIE converges very similarly: e.g. the stress concentrations are 2·781, 3·126, 3·228, 3·248 and 3·252 for the five meshes considered in the same order as listed in Table I. Using $\bar{N}(\mathbf{x}) \equiv 1$, the TBIE solution converges much less quickly and less smoothly: e.g. the corresponding stress concentration values are 2·828, 2·992, 3·249, 3·241 and 3·280.

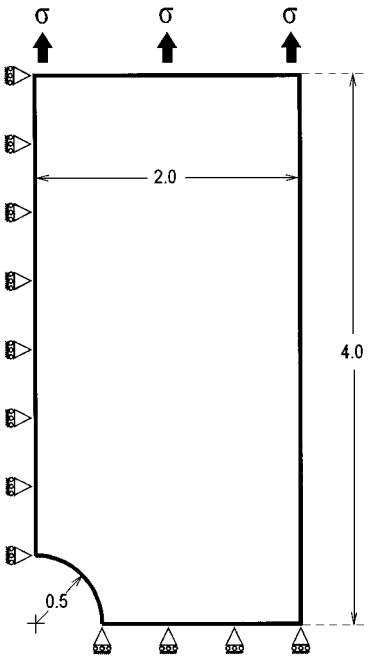

Figure 2. Rectangular solid with a central hole (one-quarter)

Table I. Solutions for a central hole in a rectangular solid

NELEM	N	ℓ	Soln.	t_2 (0·5, 0·0)	u_1 (0·5, 0·0)	u_2 (0·0, 0·5)
24	2	0·5	BIE	− 3·001	− 0·212278	0·564120
			TBIE	− 3·099	− 0·202446	0·557645
			Diff	3·3%	4·6%	1·1%
47	3	0·25	BIE	− 3·164	− 0·213817	0·565887
			TBIE	− 3·196	− 0·207184	0·571187
			Diff	1·0%	3·1%	0·9%
94	6	0·125	BIE	− 3·226	− 0·214021	0·566123
			TBIE	− 3·242	− 0·213622	0·565881
			Diff	0·5%	0·2%	< 0·1%
188	12	0·0625	BIE	− 3·246	− 0·214040	0·566142
			TBIE	− 3·251	− 0·213993	0·566109
			Diff	0·2%	< 0·1%	< 0·1%
376	24	0·03125	BIE	− 3·251	− 0·214042	0·566144
			TBIE	− 3·253	− 0·214036	0·566140
			Diff	0·1%	< 0·1%	< 0·1%

Table II. Stress intensity factors for a straight crack under internal pressure

N	ℓ/a	K/K^0 (A)	K/K^0 (B)	K/K^0 (C)
1	1·0	0·9981	0·9884	1·0726
2	0·5	0·9974	0·9950	1·1424
4	0·25	0·9990	0·9977	1·0291
8	0·125	0·9997	0·9988	1·0336
16	0·0625	1·0000	0·9993	1·0194
32	0·03125	1·0002	0·9995	1·0191

6.2. *Pressurized straight crack in an infinite solid* (2-*D*)

The two faces of a straight crack $-a \leqslant x_1 \leqslant +a$, $x_2 = 0$ are subdivided into a total of $4N$ uniform elements, each of length a/N. The crack faces are loaded by internal pressure $\mathbf{t} = (0, \pm\sigma)$, and so the mode I stress intensity factor is $K^0 = \sigma\sqrt{\pi a}$. Values $a = 1{\cdot}0$ and $\sigma = 1{\cdot}0$ are chosen for the boundary element study, and Table II shows numerical results (A) using $\bar{N}(\mathbf{x}) \equiv N^0(\xi)$, (B) using $\bar{N}(\mathbf{x}) \equiv (N^0(\xi))^2$, and (C) using $\bar{N}(\mathbf{x}) \equiv 1$. For scheme (A), all the meshes used give the stress intensity factor accurate to within 0·3 per cent, and for $N \geqslant 4$, the accuracy is within 0·1 per cent. For scheme (B), results are only slightly less accurate, while for scheme (C), the results converge in a much slower and more erratic manner.

6.3. *Inclined straight edge crack in a rectangular solid under tension* (2-*D*)

A rectangular block $0 \leqslant x_1 \leqslant b$, $-b \leqslant x_2 \leqslant \frac{3}{2}b$ contains an inclined straight crack emanating from the edge at (0, 0) and with its tip at $(a \sin\omega, a \cos\omega)$. The block is loaded in tension by

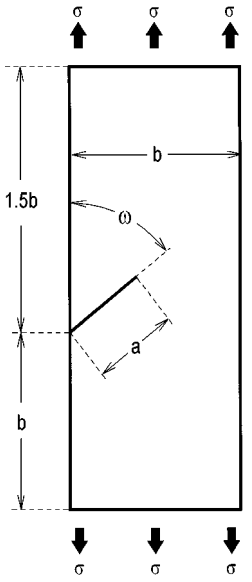

Figure 3. Inclined edge crack

Table III. Stress intensity factors for an inclined edge crack

	NELEM	32	34	64	128	256	512	Reference 10
$\omega = 45^\circ$	K_{I}	1·545	1·527	1·518	1·511	1·509	1·509	1·504
	K_{II}	0·724	0·726	0·728	0·729	0·729	0·730	0·717
$\omega = 67\frac{1}{2}^\circ$	K_{I}	2·866	2·836	2·850	2·844	2·842	2·841	2·858
	K_{II}	0·628	0·626	0·625	0·625	0·625	0·625	0·619

tractions $t_2 = +\sigma$ on $x_2 = \frac{3}{2}b$ and $t_2 = -\sigma$ on $x_2 = -b$ (see Figure 3). In the test cases, the loading is taken to be $\sigma = 1{\cdot}0$, the dimensions are chosen to be $a = 0{\cdot}5$, $b = 1{\cdot}0$, and two crack angles are considered, $\omega = 67{\cdot}5^\circ$ and $\omega = 45{\cdot}0^\circ$. References values[9] (accuracy unknown) are compared with results using the present method in Table III. The simplest element mesh used consists of 32 uniform elements of length 0·25 (including two on each crack face). Replacing each tip element with two uniform elements, each of length 0·125, gives the mesh with 34 elements. Finer meshes involve 64 uniform elements each of length 0·125 (including four elements on each crack face), 128 uniform elements each of length 0·0625, 256 uniform elements each of length 0·03125, and 512 uniform elements each of length 0·015625 (including 32 elements on each crack face). Solutions converge to values within 2 per cent of the reference values. For both crack angles, the meshes of 34 elements are adequate to give stress intensity factors to about 1 per cent of the apparent converged values, i.e. $K_{\mathrm{I}} = 1{\cdot}509$, $K_{\mathrm{II}} = 0{\cdot}730$ for $\omega = 45{\cdot}0^\circ$ and $K_{\mathrm{I}} = 2{\cdot}841$, $K_{\mathrm{II}} = 0{\cdot}625$ for $\omega = 67{\cdot}5^\circ$, given by 512 elements. Using $\bar{N}(\mathbf{x}) \equiv (N^0(\xi))^2$, the results differ from those for $\bar{N}(\mathbf{x}) \equiv N^0(\xi)$ by less than 0·4 per cent for 32 elements and are virtually identical for the other meshes. When $\bar{N}(\mathbf{x}) \equiv 1$ is used instead, convergence is very slow, e.g. for $\omega = 45{\cdot}0^\circ$, solutions differ from the above converged values by over 10 per cent with 128 elements and over 2 per cent with 512 elements.

6.4. Circular quadrant crack under remote uniaxial tension (2-*D*)

A curved crack described by the circular quadrant $x_1 = R\cos\phi$, $x_2 = R\sin\phi$ with $\frac{1}{4}\pi \leqslant \phi \leqslant \frac{3}{4}\pi$ is situated in a large solid $-L \leqslant x_1 \leqslant L$, $-L \leqslant x_2 \leqslant L$ under uniaxial tension $t_2 = \pm\sigma$ on its ends $x_2 = \pm L$ (see Figure 4). For $L \gg R$, the stress intensity factors are known exactly,[9] and values $L = 100{\cdot}0$, $R = 1{\cdot}0$ and $\sigma = 1{\cdot}0$ are chosen for the tests. Owing to the requirement that the quadratic quarter point elements at the crack tips must be straight, it is necessary to make these elements very small to approximate the curved geometry. Consequently, a set of symmetric meshes is used with element lengths defined on the crack in the ratios 1:1:2:4:8:16:16:16:*etc.* over $\frac{1}{4}\pi \leqslant \phi \leqslant \frac{1}{2}\pi$ and $\frac{3}{4}\pi \geqslant \phi \geqslant \frac{1}{2}\pi$. So with a total of $4N$ elements on both faces of the crack, the crack tip elements are of length $\ell = (\frac{1}{4}\pi R)/(16(N-4))$. Convergence of the stress intensity factors with increasing N is demonstrated in Table IV, where it can be seen that the solution is within 1·0 per cent for $N \geqslant 9$. When $\bar{N}(\mathbf{x}) \equiv (N^0(\xi))^2$ is used, values are within 0·1 per cent of those for $\bar{N}(\mathbf{x}) \equiv N^0(\xi)$, but for $\bar{N}(\mathbf{x}) \equiv 1$, convergence is very slow, with errors, of 5·5 per cent for $N = 6$ reducing to 2·0 per cent for $N = 48$.

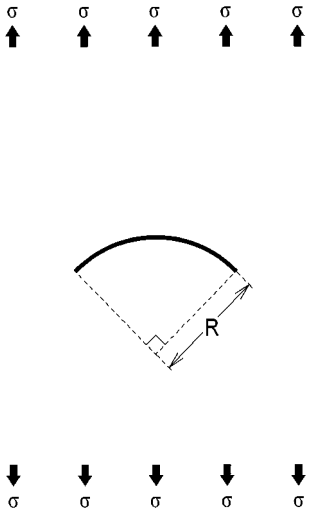

Figure 4. Circular arc crack

Table IV. Stress intensity factors for a circular quadrant crack

N	$\ell/(\frac{1}{4}\pi R)$	K_{I}	K_{II}
6	1/32	0·8253 (1·8%)	0·8983 (0·9%)
9	1/80	0·8151 (0·6%)	0·9015 (0·5%)
12	1/128	0·8126 (0·3%)	0·9023 (0·4%)
24	1/320	0·8100 (0·1%)	0·9030 (0·4%)
48	1/704	0·8091 (0·2%)	0·9035 (0·3%)
Exact (Reference 10)		0·8107	0·9062

6.5. Circumferential crack in a long cylinder under torsion and tension (3-*D*)

A solid cylinder of radius R and length $2L$, defined by the region $x_1^2 + x_2^2 \leqslant R^2$, $-L \leqslant x_3 \leqslant +L$, has a circumferential crack of depth a lying in the annular region $x_3 = 0$, $R - a \leqslant \sqrt{x_1^2 + x_2^2} \leqslant R$ (see Figure 5). The ends $x_3 = \pm L$ are loaded in torsion and tension by tractions $\mathbf{t} = (\pm qx_2/R, \mp qx_1/R, \pm \sigma)$ on $x_3 = \pm L$. The example chosen is for a deep crack $a/R = 0{\cdot}9$ in a long cylinder $R = 1{\cdot}0$ and $L = 4{\cdot}0$, and the loading is $\sigma = 1{\cdot}0$ and $q = 1{\cdot}0$. Stress intensity factors for an infinitely long cylinder, $L \gg R$, are known with accuracy reckoned to be better than 1·0 per cent and are given by[10]

$$K_{\mathrm{I}} = \tfrac{1}{2}\{1 + \tfrac{1}{2}c + \tfrac{3}{8}c^2 - 0{\cdot}363c^3 + 0{\cdot}731c^4\}c^{-3/2}\sigma\sqrt{\pi a}$$
$$K_{\mathrm{III}} = \tfrac{3}{8}\{1 + \tfrac{1}{2}c + \tfrac{3}{8}c^2 + \tfrac{5}{16}c^3 + \tfrac{35}{128}c^4 + 0{\cdot}208c^5\}c^{-5/2}q\sqrt{\pi a} \tag{54}$$

where $c = 1 - a/R$, so for the present example $K_{\mathrm{I}} = 28{\cdot}008$, $K_{\mathrm{II}} = 0$ and $K_{\mathrm{III}} = 210{\cdot}19$.

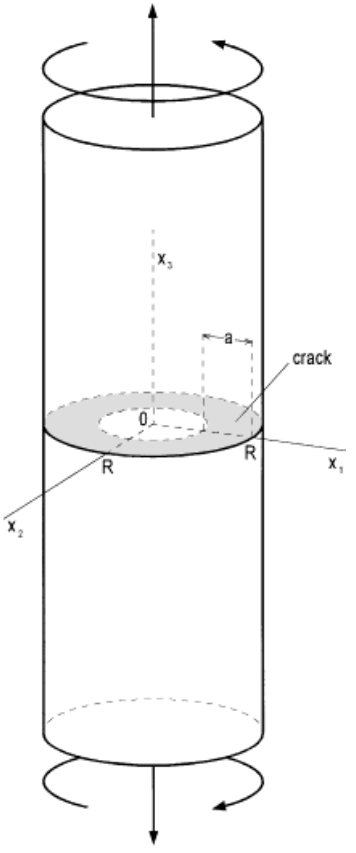

Figure 5. Edge cracked cylinder under tension and torsion

Table V. Stress intensity factors for an edge cracked cylinder

Mesh	NELEM	NNODE	K_{I}	K_{III}
A	192	738	27·50 – 27·55 (1·8%)	215·2 – 215·7 (2·6%)
B	208	802	27·71 – 27·75 (1·1%)	209·2 – 209·8 (0·5%)
C	224	866	27·85 – 27·85 (0·6%)	208·7 – 209·0 (0·7%)
D	240	930	27·95 – 27·88 (0·5%)	209·3 – 208·9 (0·6%)
	Reference 11		28·01	210·2

A symmetric mesh of elements is used, comprising eight regular angular subdivisions about the x_3-axis and six subdivisions each over $0 \leqslant x_3 \leqslant +L$ and $0 \geqslant x_3 \geqslant -L$ weighted in the ratios 3:3:6:8:10:10. Four different subdivisions of the crack in the radial direction $R - a \leqslant \sqrt{x_1^2 + x_2^2} \leqslant R$ are considered to demonstrate convergence, weighted from the crack front in the ratios 1:1:2:4:4 (mesh A), 1:1:2:4:8:8 (mesh B), 1:1:2:4:8:16:16 (mesh C) and 1:1:2:4:8:16:32:32 (mesh D). The numerical results for each of the meshes are given in Table V, and show the maximum and minimum values of stress intensity factor on the crack front, and the percentage difference from the reference solution (54). For all meshes $K_{\mathrm{II}} < 10^{-5}$, and the values of K_{I} and K_{III} vary by less than 0·3 per cent along the crack front and converge steadily towards the reference values as the number of elements is increased, with errors of less than 1 per cent for meshes C and D. Using $\bar{N}(\mathbf{x}) \equiv (N^0(\xi))^2$ gives slightly less accurate results, with 5·9 per cent errors for mesh A reducing to 1·0 per cent for mesh D. In this example, the numerical method using $\bar{N}(\mathbf{x}) \equiv 1$ fails completely: solutions are wildly inaccurate (80 per cent errors for mesh D) and there is no evidence of any tendency to converge.

7. DISCUSSION

The nature of hypersingular boundary integral equations and the resulting implications for what constitutes a valid numerical solution method has received attention from many authors (e.g. see References 1, 2, 5, 6, 11–13 and references therein). There is common agreement that some kind of continuity condition concerning displacement gradients is required for the singular integrals in the BIDE and the TBIE to exist on parts of the boundary which include the source point. When the source point is on a smooth part of the boundary, it is sufficient to ensure that the traction and the tangential gradients of displacement are each continuous at the source point.[6] However, the general form of this condition cannot depend simply up on continuity of traction and tangential gradients of displacement in isolation, since these quantities are necessarily discontinuous at corner points. The coefficients of potentially log-singular terms in the BIDE can be shown to involve linear combinations of traction and tangential gradients of displacement,[1] and it may be inferred that the general form of the continuity condition must involve values of traction and tangential derivatives of displacement connected by the identity (13). It is this connection between the surface displacement and traction that allows direct evaluation of the singular boundary integrals by using Stokes' theorem. Some consequences of this approach for elastostatics and its implementation in a numerical boundary element method are discussed below.

7.1. Cancellation of singularities

The analytical treatment of singular integrals using Stokes' theorem gives a useful perspective on the precise form of the singularities in the BIDE, especially for the 2-D case where the log-singular free terms $B_{pqjk}u^0_{p,q}$ are evaluated in closed-form. The boundary integrals B_{pqjk} are converted into expressions evaluated on the perimeter of each section of the boundary on which the displacement gradients are unique (continuous) at the source point and compatible with the local tractions (13). These source point conditions are automatically satisfied on each individual piecewise smooth boundary element, where the unique tangential gradients of the assumed displacement are independent of the normal gradients implicit in the unique traction. However, for a boundary source point on the perimeter of an element (e.g. at a corner), the coefficients B_{pqjk} are log-singular, and the BIDE does not exist unless all such singularities exactly cancel out. The cancellation of singular terms may be illustrated using the closed-form expressions (45) for the 2-D case, where the log-singular parts of the BIDE contained in the free terms $B_{pqjk}u^0_{p,q}$ are of the form $b_{jk}\log r$, where

$$b_{jk} = \frac{-1}{8\pi(1-\nu)}\left\{(3-4\nu)\delta_{pj}\varepsilon_{qk3} + \delta_{qj}\varepsilon_{pk3} + \frac{2(1-\nu)}{1-2\nu}\,\delta_{pq}\varepsilon_{jk3}\right\}\Delta u^0_{p,q} \tag{55}$$

and $\Delta u^0_{p,q}$ denotes the difference between the displacement gradients assumed on elements either side of the source point. The individual components reduce to

$$\begin{aligned}
b_{11} &= \frac{1}{8\pi(1-\nu)}\left\{(3-4\nu)\Delta u^0_{1,2} + \Delta u^0_{2,1}\right\}\\
b_{22} &= \frac{-1}{8\pi(1-\nu)}\left\{(3-4\nu)\Delta u^0_{2,1} + \Delta u^0_{1,2}\right\}\\
b_{12} &= \frac{-1}{8\pi}\left\{4\Delta u^0_{1,1} + \frac{2}{1-2\nu}\,(\Delta u^0_{1,1} + \Delta u^0_{2,2})\right\}\\
b_{21} &= \frac{1}{8\pi}\left\{4\Delta u^0_{2,2} + \frac{2}{1-2\nu}\,(\Delta u^0_{1,1} + \Delta u^0_{2,2})\right\}
\end{aligned} \tag{56}$$

For a source point $r = 0$ at the junction of two elements, it may be seen that the singular terms $b_{jk}\log r$ cancel out only if all the displacement gradients $u^0_{p,q}$ are unique, so that $\Delta u^0_{p,q} = 0$. Expressed in terms of conditions pertaining to the surface variables, the existence of the BIDE requires the following: *the forms of displacement and traction assumed on all boundary elements adjoining the source point must be exactly consistent with unique displacement gradients at the source point*. Using the special interpolations (21) and (22) guarantees this, and the $O(\log r)$ expressions included in B_{pqjk} need be evaluated only on the remote perimeter of the entire set of elements adjoining the source point. The formulae for boundary stress (47) and the TBIE (48) derived from the BIDE (46) are based on the existence of B_{pqjk}, and therefore require the same continuity conditions as the BIDE.

7.2. The stress boundary integral equation (SBIE)

The SBIE may be defined from the BIDE by the operation $E_{ijkl}I_{kl}(\mathbf{x}^0, S)$, with E_{ijkl} given by (14). For $\mathbf{x}^0$ interior to S, the SBIE gives the stress $\sigma_{ij}(\mathbf{x}^0) = E_{ijkl}I_{kl}(\mathbf{x}^0, S)$, and in 2-D there

are three independent components of the SBIE (since $E_{12kl} = E_{21kl}$). The SBIE for $\mathbf{x}^0$ on the boundary S may be derived as a special case from the present analysis for the BIDE, and the free terms in the SBIE are of the form $E_{ijkl}B_{pqkl}u^0_{p,q}$. These free terms involve log-singularities, which for 2-D are

$$c_{rs}\log r \equiv E_{rsjk}b_{jk}\log r = \{\lambda\delta_{rs}(b_{11}+b_{22}) + \mu(b_{rs}+b_{sr})\}\log r \tag{57}$$

so that the individual components are

$$\begin{aligned}
c_{11} &= \frac{1}{4\pi(1-\nu)}\,\mu\{(\Delta u^0_{1,2} - \Delta u^0_{2,1}) + 2(1-\nu)(\Delta u^0_{1,2} + \Delta u^0_{2,1})\} \\
c_{22} &= \frac{1}{4\pi(1-\nu)}\,\mu\{(\Delta u^0_{1,2} - \Delta u^0_{2,1}) - 2(1-\nu)(\Delta u^0_{1,2} + \Delta u^0_{2,1})\} \\
c_{12} &= c_{21} = \frac{1}{2\pi}\,\mu\{\Delta u^0_{2,2} - \Delta u^0_{1,1}\}
\end{aligned} \tag{58}$$

It can be seen that the continuity conditions at a boundary source point required for the SBIE to exist relate to the three combinations of the displacement gradients $(u^0_{2,2} - u^0_{1,1})$, $(u^0_{1,2} + u^0_{2,1})$ and $(u^0_{1,2} - u^0_{2,1})$. Notice that continuity of stress, corresponding to continuity of only the symmetric combinations $(u^0_{p,q} + u^0_{q,p})$, is not sufficient for the SBIE to exist.

At a corner point $\mathbf{x}^0$, the free terms in the SBIE do not involve only symmetric (strain) combinations of $u^0_{p,q}$, from which the stress components are defined. There also exist antisymmetric (non-strain or rotation) displacement gradients, e.g. $u^0_{1,2} - u^0_{2,1}$, so that if the SBIE is to be used to determine stress values on the boundary, then these non-strain gradients must be approximated in terms of the boundary traction and displacement (as described in Section 5). Compare this with the integral formula for evaluating boundary stresses given by (46) and (47), i.e. $E_{ijrs}Q_{klrs}I_{kl}(\mathbf{x}^0, S) = 0$, in which the gradient-related free terms are reduced to pure stress components (47). A TBIE may formulated directly from the SBIE,[2,6] instead of from the BIDE as in the present approach. It might be expected that the TBIE derived from the BIDE specifically to give free terms involving strong crack pressure terms (50) or only tractions (48) would perform better than that derived from the SBIE, i.e. $\hat{n}_j E_{ijkl}I_{kl}(\mathbf{x}^0, S) = 0$ in which there is no freedom to choose the form of the free terms. However, for the examples in Section 6 earlier, it is found that both formulae for the TBIE give very similar numerical solutions, and there is no clear practical evidence for an optimum definition of the TBIE.

7.3. Regularization of the equation

In the present approach, displacement gradient continuity conditions are incorporated directly into the assumed forms of the boundary displacement and traction by way of the special interpolations (21) and (22). However, the resulting non-singular BIDE (23) may alternatively be regarded as being derived from a direct regularization of the basic hypersingular form of the BIDE (4), obtained by adding on an extra integral term which ensures cancellation of the

log-singularities arising at the source point

$$I_{jk}(\mathbf{x}^0; S) = \int_S \{T_{ijk}(\mathbf{x}, \mathbf{x}^0)\bar{u}_i(\mathbf{x}) - U_{ijk}(\mathbf{x}, \mathbf{x}^0)\bar{t}_i(\mathbf{x})\}\, \mathrm{d}S(\mathbf{x})$$
$$+ \int_{\Delta S} \{(u^0_{p,q} - \bar{u}_{p,q}(\mathbf{x}^0))\rho_q T_{pjk}(\mathbf{x}, \mathbf{x}^0) \tag{59}$$
$$- (n^0_s E_{ispq} u^0_{p,q} - \bar{t}_i(\mathbf{x}^0)) U_{ijk}(\mathbf{x}, \mathbf{x}^0)\} \bar{N}(\mathbf{x})\, \mathrm{d}S(\mathbf{x}) = 0$$

where $\bar{u}_{i,j}(\mathbf{x})$ and $\bar{t}_i(\mathbf{x})$ may be discontinuous and incompatible at $\mathbf{x}^0$. In effect, the extra integral over ΔS in (59) is a weighted residual which forces $\bar{u}_i(\mathbf{x})$ and $\bar{t}_i(\mathbf{x})$ to converge towards a solution which complies with the required continuity conditions involving unique displacement gradients $u^0_{p,q}$ at $\mathbf{x}^0$. It can be seen that equations (23) and (59) are identical, and therefore that variable regularization and equation regularization[2] are essentially equivalent. However, regarded in this way, it is not obvious why the weight function $\bar{N}(\mathbf{x}) \equiv 1$ should give a less robust numerical method than $\bar{N}(\mathbf{x}) \equiv N^0(\xi)$, as was demonstrated in the examples earlier. On the other hand, variable regularization, as in (21) and (22), demands not only that $\bar{N}(\mathbf{x}^0) = 1$ at the source point, but also that $\bar{N}(\mathbf{x}) = 0$ at the non-source nodes on each element to avoid any mismatch between the modified interpolations (21) and (22) and the nodal values of displacement and traction.

7.4. Inconsistency of interpolation scheme

In the conventional boundary element method, definitive interpolations $\bar{u}_i(\xi)$ and $\bar{t}_i(\xi)$ are assumed over each element for every collocation (source) point. The resulting numerical solution of the BIE, in the form of a discrete set of nodal values, may be interpreted as representing a definite continuous solution over the entire boundary by applying the interpolations $\bar{u}_i(\xi)$ and $\bar{t}_i(\xi)$ on each element. However, the conventional method is not valid for solution of the TBIE. In the present approach, different forms of interpolation are used on a given element depending on the circumstances: i.e. when the source point does not lie on the element, $\bar{u}_i(\xi)$ and $\bar{t}_i(\xi)$ are used; otherwise (21) and (22) are used, which depend upon the position of the source point on the element. Consequently, when the TBIE is reduced to a set of numerical equations by collocating at nodal points on continuous elements, no definitive scheme exists to interpret the discrete solution at points between nodes on the boundary. Although this inconsistency is unorthodox, the interpolation scheme leads to a perfectly valid numerical method in which the discrete set of nodal displacement and traction values converges smoothly to the correct solution as more boundary elements are used. Notice however that if the form of the TBIE is regarded as an equation regularization,[2] as in the BIDE (59), then $\bar{u}_i(\xi)$ and $\bar{t}_i(\xi)$ may be regarded as a definitive boundary interpolation.

8. CONCLUSIONS

A non-singular formulation for the BIDE has been developed and provides the basis for a numerical method for the TBIE using continuous boundary elements for 2-D and 3-D elastostatics. Subtle modifications are made to the displacement and traction interpolations used on boundary elements adjoining the source point, which enforce exactly the continuity conditions necessary for the BIDE and the TBIE to exist. These conditions are that the displacement

gradients must be unique and compatible with all local tractions at the source point. Parameters representing the unique displacement gradients at the source point are introduced into the BIDE for this purpose, and are later expressed in terms of the surface traction and displacement when the BIDE is reduced to the TBIE.

By taking radial series expansions of the surface displacement and traction about the source point in the BIE and BIDE, coefficients of displacement and displacement gradient at the source point are isolated and expressed in forms which allow application of Stokes' integral theorem. Direct evaluation of the source term coefficients is essential for a single-domain boundary integral equation method for crack problems, and the present approach leads to non-singular forms of the equations, which require no reference to singular integrals or Cauchy/Hadamard principal values. A procedure for constructing a numerically robust TBIE from the BIDE is given for general 2-D problems; the corresponding procedure for 3-D is given in Reference 1.

Numerical solutions of the TBIE using continuous boundary elements are presented to demonstrate the application of the present method, including some for curved cracks and edge cracks, all obtained using continuous boundary elements. It is demonstrated that numerical solutions from the TBIE converge satisfactorily, and that the method is capable of treating general crack problems. Stress intensity factors are calculated from the crack opening displacement on quarter point elements at the crack front, and values obtained are typically accurate to within 1 per cent.

REFERENCES

1. A. Young, 'A single domain boundary element method for 3-D elastostatic crack analysis using continuous elements', *Int. J. Numer. Meth. Engng.*, **39,** 1265–1293 (1996).
2. Q. Huang and T. A. Cruse, 'On the non-singular traction-BIE in elasticity', *Int. J. Numer. Meth. Engng.*, **37,** 2041–2072 (1994).
3. T. A. Cruse and W. Suwito, 'On the Somigliana stress identity in elasticity', *Comput. Mech.*, **11,** 1–10 (1993).
4. V. Mantic, 'A new formula for the *C*-matrix in the Somigliana identity', *J. Elasticity*, **33,** 191–201 (1993).
5. G. Krishnasamy, L. W. Schmerr, T. J. Rudolphi and F. J. Rizzo, 'Hypersingular boundary integral equations: some applications in acoustic and elastic wave scattering', *J. Appl. Mech.*, **57,** 404–414 (1990).
6. A. Portela, M. H. Aliabadi and D. P. Rooke, 'The dual boundary element method: effective implementation for crack problems', *Int. J. Numer. Meth. Engng.*, **33,** 1269–1287 (1992).
7. P. K. Bannerjee and R. Butterfield, *Boundary Element Methods in Engineering Science*, 1st edn, McGraw-Hill, Maidenhead, 1981.
8. R. E. Peterson, *Stress Concentration Factors*, Wiley, New York, 1974.
9. D. P. Rooke and D. J. Cartwright, *Compendium of Stress Intensity Factors*, HMSO, 1976.
10. J. P. Benthem and W. T. Koiter, 'Asymptotic expansions to crack problems', in *Mechanics of Fracture 1*: *Methods of Analysis and Solutions of Crack Problems* G. C. Sih (ed.), Noordhoff International Publishing, Leyden, 1973.
11. M. Guiggiani, G. Krishnasamy, T. J. Rudolphi and F. J. Rizzo, 'A general algorithm for the numerical solution of hypersingular boundary integral equations', *J. Appl. Mech.*, **59,** 604–614 (1992).
12. P. A. Martin and F. J. Rizzo, 'Hypersingular integrals: how smooth must the density be?', *Int. J. Numer. Meth. Engng.*, **39,** 687–704 (1996).
13. J. T. Chen and H.-K. Hong, 'Dual boundary integral equations at a corner using contour approach around singularity', *Adv. Eng. Software*, **21,** 169–178 (1994).